Characterization of heterogeneous fracture compliance using multiple reflections coupled with data-driven Green's function retrieval

Shohei Minato and Ranajit Ghose, Delft University of Technology*

SUMMARY

The spatial heterogeneity along a fracture is a key determinant for fracture-associated hydraulic properties. We propose a new method to estimate the heterogeneous compliance distribution of a fracture from the reflection response at the fracture surface. For this purpose, we formulate a data-driven approach for Green's function retrieval based on Marchenko equation coupled with the inverse scattering to solve the linear-slip boundary condition. The approach estimates the wavefield along the fracture accurately, including the multiple reflections. Furthermore, it offers the opportunity to estimate compliance using multiple reflections, which was not possible so far. We show this concept by numerically modeling 2D SH waves sensing the heterogeneous tangential compliance of a fracture. Our results show that the use of multiple reflections leads to a better estimation of the heterogeneous fracture compliance than using primary reflection alone, especially for the far offsets on the fracture plane.

INTRODUCTION

The defects in solid materials, like fractures, are often represented as linear-slip boundaries or non-welded interface across which the stress is continuous but the displacement is discontinuous (e.g., Schoenberg, 1980; Pyrak-Nolte et al., 1990; Wapenaar et al., 2004). Characterizing the spatially heterogeneous fracture compliance through use of elastic waves has the potential to illuminate the hydraulic properties along a fracture. Furthermore, the spatial heterogeneity of fracture compliance is important in order to address the apparent frequency dependence of compliance in the laboratory scale as well as in the field-seismic scale (Biwa et al., 2007; Worthington and Lubbe, 2007; Baird et al., 2013).

Recently, we have formulated the inverse scattering problem to estimate the heterogeneous compliance distribution along a fracture using the scattered elastic wavefield (Minato and Ghose, 2013, 2014a). The method requires two steps: (1) locating the position of the fracture, and (2) estimating the stress field along the fracture to solve the linear-slip boundary condition. With a homogeneous compliance model, Minato and Ghose (2013, 2014a) have shown that the imaging (step 1) and wavefield estimation along fracture (step 2) are possible using the backpropagation of reflection responses. However, for a more complex background medium a new method is required to handle accurately the effect of multiple reflections. In this vein, we have derived a nonlinear imaging condition in order to image accurately single and multiple fractures using multiple scattered waves (Minato and Ghose, 2014b, 2015).

Wapenaar et al. (2014a,b) have presented a new method for retrieving the Green's function inside a medium using reflection responses at the surface of the earth. The method solves Marchenko equation and constructs the Green's function including multiple reflections. Using the method for the characterization of heterogeneous fracture is beneficial because it enables estimating the wavefield along the fracture plane (step 2) accurately handling the multiple reflections without requiring the detailed subsurface information. Furthermore, it gives us a possibility to characterize the heterogeneous compliance using the multiple reflections, which has not been possible so far.

In this study, we apply the data-driven Green's function retrieval using Marchenko equation in order to retrieve the wavefield along the fracture plane. Furthermore, we characterize the heterogeneous fracture compliance using retrieved primary and multiple reflections. We first briefly discuss the data-driven Green's function retrieval approach and use of inverse scattering to estimate the heterogeneous fracture compliance. Next, we show numerically the effectiveness of this new method. In this study, we use 2D SH wave because (1) in this case the elastic wavefield senses the tangential component of the fracture compliance (tangential compliance, η_T), and (2) the simple scalar wavefield offers essential insights on this new concept.

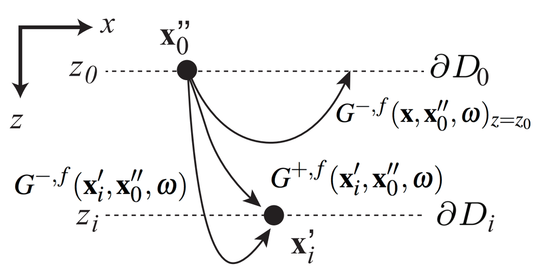

Figure 1: Configuration for data-driven Green's function retrieval. Virtual receiver responses at $\partial \mathbf{D}_i$ from the reflection responses at the measurement surface $\partial \mathbf{D}_0$, retrieved as decomposed upgoing ($-$) and downgoing ($+$) Green's function.

THEORY

Data-driven Green's function retrieval using Marchenko equation

Here we create virtual receivers right on the heterogeneous fracture from the surface seismic measurements. We assume that locating the fracture has been possible using a-priori processing steps, e.g., migration of reflected waves (Minato and Ghose, 2014a, 2015). Next, we briefly explain the new approach of data-driven Green's function retrieval using the Marchenko equation. We have modified for 2D SH wave configuration the 3D approach for acoustic media (Wapenaar et al., 2014a,b). Therefore, $\mathbf{x} = (x,z)$ points a position vector in x-z plane and the two-way Green's function $G^{v_y,f}$ is defined as a

DOI http://dx.doi.org/10.1190/segam2015-5845404.1

particle velocity in y direction (v_y) due to a point force in y direction (f). The data-driven Green's function retrieval using Marchenko equation is an iterative procedure to estimate the up- and downgoing parts of the so-called focusing function ($f_1^{\pm}$ and its coda part M^+) which focuses at $\mathbf{x}_i'$ on the surface $\partial\mathbf{D}_i$ below the measurement surface (Figure 1):

$$M_k^+(\mathbf{x}_0'',\mathbf{x}_i',-t) = \int_{\partial\mathbf{D}_0} d\mathbf{x}_0 \int_{-t_d^{\varepsilon}(\mathbf{x}_i',\mathbf{x}_0)}^{t} R(\mathbf{x}_0'',\mathbf{x}_0,t-t') f_{1,k}^-(\mathbf{x}_0,\mathbf{x}_i',-t')dt', \quad (1)$$

$$f_{1,k+1}^-(\mathbf{x}_0'',\mathbf{x}_i',t) = f_{1,0}^-(\mathbf{x}_0'',\mathbf{x}_i',t) + \int_{\partial\mathbf{D}_0} d\mathbf{x}_0 \int_{-t_d^{\varepsilon}(\mathbf{x}_i',\mathbf{x}_0)}^{t} R(\mathbf{x}_0'',\mathbf{x}_0,t-t') M_k^+(\mathbf{x}_0,\mathbf{x}_i',t')dt', \quad (2)$$

$$f_{1,0}^-(\mathbf{x}_0'',\mathbf{x}_i',t) = \int_{\partial\mathbf{D}_0} d\mathbf{x}_0 \int_{-\infty}^{-t_d^{\varepsilon}(\mathbf{x}_i',\mathbf{x}_0)} R(\mathbf{x}_0'',\mathbf{x}_0,t-t') T_d^{inv}(\mathbf{x}_i',\mathbf{x}_0,t')dt', \quad (3)$$

where the reflection response R is defined as the responses with sources and receivers on the measurement surface $\partial\mathbf{D}_0$ (Figure 1), with $R(\mathbf{x}_0'',\mathbf{x}_0,\omega) = (1/2j\omega\mu^{-1})^{-1}\partial_z G^{-,f}(\mathbf{x},\mathbf{x}_0'',\omega)_{z=z_0}$. We approximate the inverse of the transmission response T_d^{inv} to be its direct arrival, as $T_d^{inv}(\mathbf{x}_i',\mathbf{x}_0'',t) \approx G_d(\mathbf{x}_i',\mathbf{x}_0'',-t)$.

Once we estimate the focusing functions assuming the iteration converges, we can retrieve the up- and downgoing Green's functions recorded at the virtual receiver ($\mathbf{x}_i'$) located inside the medium ($\partial\mathbf{D}_i$) from the source located on the measurement surface ($\partial\mathbf{D}_0$):

$$G^{+,f}(\mathbf{x}_i',\mathbf{x}_0'',t) = f_1^+(\mathbf{x}_0'',\mathbf{x}_i',-t) - \int_{\partial\mathbf{D}_0} d\mathbf{x}_0 \int_{-\infty}^{t} R(\mathbf{x}_0'',\mathbf{x}_0,t-t') f_1^-(\mathbf{x}_0,\mathbf{x}_i',-t')dt', \quad (4)$$

$$G^{-,f}(\mathbf{x}_i',\mathbf{x}_0'',t) = -f_1^-(\mathbf{x}_0'',\mathbf{x}_i',t) + \int_{\partial\mathbf{D}_0} d\mathbf{x}_0 \int_{-\infty}^{t} R(\mathbf{x}_0'',\mathbf{x}_0,t-t') f_1^+(\mathbf{x}_0,\mathbf{x}_i',t')dt', \quad (5)$$

where the focusing function f_1^+ can be constructed by its coda part, as $f_{1,k}^+(\mathbf{x}_0'',\mathbf{x}_i',t) = T_d^{inv}(\mathbf{x}_i',\mathbf{x}_0'',t) + M_{k-1}^+(\mathbf{x}_0'',\mathbf{x}_i',t)$.

These equations exploit the causality of the Green's functions. Therefore, we require the travel time of the first arrivals - $\mathbf{x}_i'$ and $\mathbf{x}_0''$ as $t_d(\mathbf{x}_i',\mathbf{x}_0'')$ and the corresponding muting function $t_d^{\varepsilon} = t_d - \varepsilon$, where ε is a small positive constant. Furthermore, due to causality, we have the relation $M_k^+(\mathbf{x}_0'',\mathbf{x}_i',-t) = f_{1,k+1}^-(\mathbf{x}_0'',\mathbf{x}_i',t) = 0$ for $t \geq t_d(\mathbf{x}_i',\mathbf{x}_0'')$. Note that the retrieved up- and downgoing Green's functions are related to the two-way Green's function as $G^{v_y,f} = G^{+,f} + G^{-,f}$.

Characterizing heterogeneous fracture compliance

Having retrieved the virtual receiver responses at positions $\mathbf{x}_i'$ on the fracture plane, we can then estimate the heterogeneous fracture compliance by directly using the method presented in Minato and Ghose (2013, 2014a). These earlier studies consider only primary reflections in a homogeneous medium. However, the formulation is valid for multiply reflected waves as long as the radiation condition in the bottom layer is sufficient. Characterization using multiple reflections is now possible because the Green's function retrieved using the Marchenko approach correctly includes those multiple reflections. Here we adapt the formulation of Minato and Ghose (2013, 2014a) for 2D SH waves.

The retrieved Green's function $G^{\pm,f}$ from equation 4 and 5 is in the form of particle velocity v_y. We can estimate corresponding stress field as:

$$\hat{\tau}_{yz}^{\pm}(\omega,k_x) = \pm\frac{\mu k_{z,s}}{\omega}\hat{v}_y^{\pm}(\omega,k_x), \quad (6)$$

where $k_{z,s} = \sqrt{(\omega/V_S)^2 - k_x^2}$ and $\Im(k_{z,s}) \leq 0$. Once the stress field along the fracture plane is estimated, one can estimate the heterogeneous compliance distribution. This requires solving the linear-slip boundary condition as represented in the frequency-wavenumber domain (Minato and Ghose, 2013), assuming the radiation condition in the bottom medium to be:

$$\hat{A}(\omega,k_x) = i\omega\eta_T(k_x) * \hat{B}(\omega,k_x), \quad (7)$$

where $*$ denotes convolution in the wavenumber domain. The function $\hat{A}$ and $\hat{B}$ are calculated from the stress field at the fracture as

$$\hat{A} = -\frac{2\omega}{\mu k_{z,s}}\hat{\tau}_{yz}^-, \quad (8)$$

$$\hat{B} = \hat{\tau}_{yz}^- + \hat{\tau}_{yz}^+. \quad (9)$$

After inverse Fourier transformation, we obtain the heterogeneous compliance distribution as,

$$\eta_T(x) = \frac{A(\omega,x)}{i\omega(1+\varepsilon^{reg}/|B(\omega,x)|)B(\omega,x)}, \quad (10)$$

where ε^{reg} is a regularization factor to stabilize the solution.

NUMERICAL MODELING

Using 2D numerical modeling, we demonstrate the concept of data-driven Green's function retrieval with the Marchenko equation and the characterization of the heterogeneous fracture compliance.

Retrieval of response along fracture plane

We consider two elastic half spaces which include a single heterogeneous fracture in the second layer (Figure 2). The source and receiver arrays are installed in the first layer. The two boundaries create multiple reflections which impinge on the fracture multiple times. This simple model offers useful insights on the concept that we propose here.

The heterogeneous fracture is represented by a random variation in the tangential compliance along a large fracture with length 1000 m. 451 point sources and 451 receivers are installed with a spacing of 4 m. We model the responses in the frequency-wavenumber domain using the wdSDD method (Nakagawa et al., 2004; Minato and Ghose, 2013), modified to include an extra layer. Figure 3a shows the modeled reflection response R due to the source located at the center of the array. A Ricker wavelet of 40 Hz centre frequency has been convolved. The primary arriving event is a reflection from

DOI http://dx.doi.org/10.1190/segam2015-5845404.1

the boundary of two elastic layers, i.e., from the welded interface. The secondary arriving event is a reflection from the heterogeneous fracture (non-welded interface). Due to the lateral heterogeneity of this interface, we see that the reflection amplitudes are heterogeneous along the receivers and scattered waves are generated. Furthermore, the multiple reflections between the welded and the non-welded interfaces arrive later on. For data-driven Green's function retrieval, we require an estimate of the direct Green's function (G_d) due to the source located inside of the medium, which will be at the position of the virtual receiver (equations 1 to 3). We calculate this assuming that the entire space is same as the first layer (Figure 3b). Therefore, we do not require the detailed structure between the measurement surface and the fracture plane. The dotted lines in Figure 3b are picked first arrivals used as t_d^{ϵ} in equations 1 to 3.

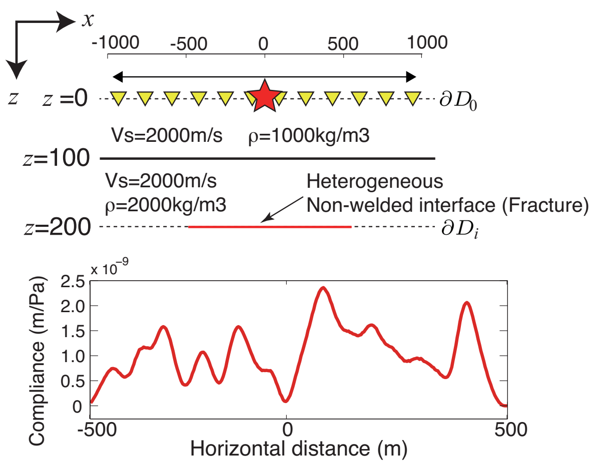

Figure 2: Fractured elastic layer and source-receiver distribution on a vertical plane. A 1000 m long fracture with heterogeneous tangential compliance distribution is considered.

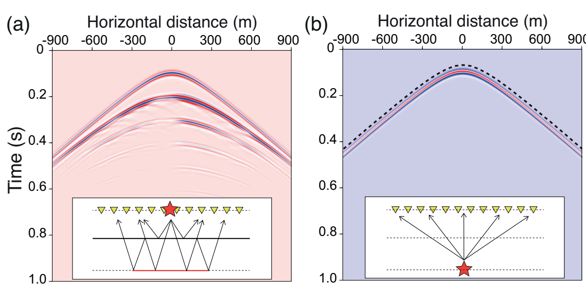

Figure 3: (a) Modeled reflection response R. (b) Direct waves G_d from the source at the virtual receiver modeled, assuming a homogeneous medium.

Figure 4 shows the retrieved wavefield using the Marchenko approach. The wavefield is retrieved as a common receiver gather with the virtual receiver created at the center of the fracture (see insets of Figure 4 for source-receiver configuration). Note that only one iteration is sufficient for convergence, for this simple model. The retrieved downgoing waves (Figure 4b) consist of the incident wave from the source at the earth's surface and the multiple reflections which are incident on the fracture from above. The retrieved upgoing waves (Figure 4a) are the reflections from the heterogeneous fracture of the downgoing (incident and multiply reflected) waves. Therefore, these wavefields correspond to a situation when a virtual receiver is installed just above the fracture plane. The directly modeled results are overlain in Figure 4a and 4b. The method could retrieve the wavefield reasonably well, especially for the near-offset data. This can be seen in the difference section in Figure 4c and 4d. Retrieving the far-offset data requires a larger source and receiver aperture. Furthermore, the first arriving events are found to be slightly erroneous, possibly because of the use of a muting function (t_d^{ϵ}) which is not optimal, thus damaging the retrieved first arrivals. Note that we calculate the difference section after applying a constant scaling factor to the retrieved wavefield. Our retrieved wavefield has larger amplitudes than in the direct modeling results, because the retrieved wavefield is biased by the input direct wave (G_d), and we calculate G_d assuming the elastic property of the first layer and ignoring the transmission effect of the welded interface. One can see that this bias, however, will be canceled to some extent in the deconvolution procedure involved in the characterization method, shown in the next subsection.

We repeat the procedure and create the virtual receivers at multiple positions along the fracture plane. Figure 5 is same as Figure 4, but for a common shot gather with the source at the center of the array and the virtual receivers located along the fracture plane. As in the retrieved common receiver gather (Figure 4), the method retrieved the wavefield well, especially for near-offset data.

Characterizing heterogeneous fracture

We use the common shot gathers retrieved in the previous subsection (Figure 5) as input data for heterogeneous fracture characterization (equations 6 to 10). We first use only the primary reflection (windowing the first arrivals in Figure 5) to estimate compliance distribution along the fracture plane. Because we solve the linear-slip boundary condition in each frequency, we can estimate the heterogeneous tangential compliance at each frequency (Figure 6a). Figure 6b shows the estimated tangential compliance at 50 Hz. One can see that the retrieved primary reflection has estimated reasonably well the true compliance distribution, especially in the near-offset. The compliance in the middle to far offset has an amplitude close to the true value, but it appears to be noisy. This is because the estimation of compliance is sensitive to the phase information of the input wave. The shape of the wavelet is possibly slightly affected during the retrieval process and this has caused this noise. Next, we use only multiple reflections as input data (windowing all events including and below the secondary arriving events in Figure 5) to estimate the compliance distribution (Figure 6c). One can see that the estimated compliance using multiple reflections are less noisy than the result using only primary reflections. Furthermore, the compliance value at 400 m is better estimated. This is because the primary reflections from this point of fracture has larger incident angles ($\approx 64^{\circ}$), and we require larger source-receiver array to correctly capture them. On the other hand, the multiply reflected

DOI http://dx.doi.org/10.1190/segam2015-5845404.1

waves from this point have smaller incident angles (with our model and the source-receiver configuration) and require less array length than while using the primaries. Finally, we stack all common shot gathers retrieved in the previous subsection and create the pseudo-plane (Gaussian) wave response along the fractures. As we exploit the enhanced near-offset response and the multiple reflections, the estimated compliance distribution is remarkably accurate at all positions on the fracture plane (Figure 6d).

CONCLUSION

We have proposed a new method to characterize the heterogeneous fracture compliance using multiple reflections, by coupling the procedure with data-driven Green's function retrieval. The 2D numerical examples show that the wavefield along the fracture plane is well retrieved except for the far-offsets and around the first arriving events, without requiring the detailed structure between the measurement surface and the fracture plane. The use of the retrieved multiple reflections leads to a much better estimation of the heterogeneous fracture compliance than from primary reflections alone. The compliance estimated from pseudo-plane-wave response using all retrieved shot gathers is very accurate because of exploiting the enhanced near-offset responses and the multiple reflections.

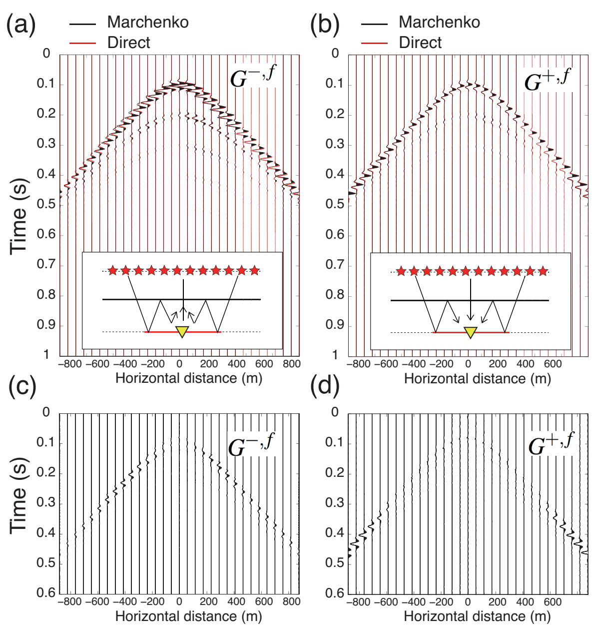

Figure 4: (a) Directly modeled and the retrieved upgoing Green's functions at a virtual receiver located right on the fracture plane. (b) Same as (a) but for the downgoing Green's function. (c) The difference between directly modeled and the retrieved upgoing Green's functions. (d) Same as (c) but for the downgoing Green's function.

ACKNOWLEDGMENTS

This work is supported by The Netherlands Research Centre for Integrated Solid Earth Science.

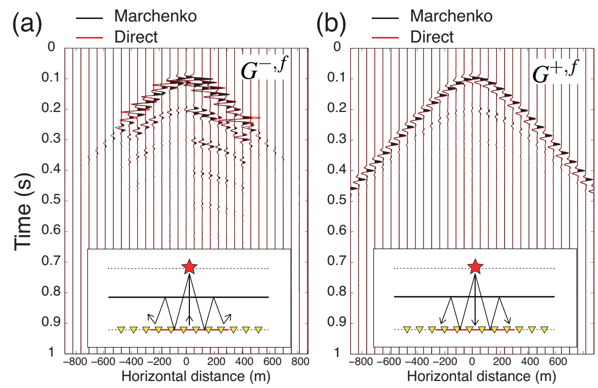

Figure 5: Same as Figure 4a and 4b but for a common shot gather after retrieving the virtual receiver responses at multiple positions on the fracture plane.

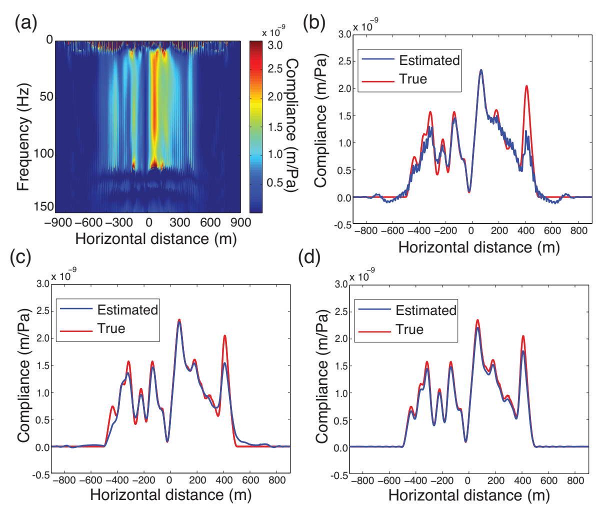

Figure 6: (a) Estimated tangential compliance using the retrieved primary reflections. (b) The result at 50 Hz in (a). (c) Same as (b) but using the retrieved multiple reflections. (d) Same as (b) but using the entire wavefield in the retrieved pseudo-plane-wave response.

DOI http://dx.doi.org/10.1190/segam2015-5845404.1

EDITED REFERENCES

Note: This reference list is a copyedited version of the reference list submitted by the author. Reference lists for the 2015 SEG Technical Program Expanded Abstracts have been copyedited so that references provided with the online metadata for each paper will achieve a high degree of linking to cited sources that appear on the Web.

REFERENCES

Baird, F., J. Kendall, and D. Angus, 2013, Frequency-dependent seismic anisotropy due to fractures: Fluid flow versus scattering: Geophysics, **78**, no. 2, WA111–WA122. http://dx.doi.org/10.1190/geo2012-0288.1.

Biwa, S., S. Hiraiwa, and E. Matsumoto, 2007, Stiffness evaluation of contacting surfaces by bulk and interface waves: Ultrasonics, **47**, no. 1–4, 123–129. http://dx.doi.org/10.1016/j.ultras.2007.08.005 PMID:17967470

Minato, S., and R. Ghose, 2013, Inverse-scattering solution for the spatially heterogeneous compliance of a single fracture: Geophysical Journal International, **195**, no. 3, 1878–1891. http://dx.doi.org/10.1093/gji/ggt348.

Minato, S., and R. Ghose, 2014a, Imaging and characterization of a subhorizontal nonwelded interface from point source elastic scattering response: Geophysical Journal International, **197**, no. 2, 1090–1095. http://dx.doi.org/10.1093/gji/ggu037.

Minato, S., and R. Ghose, 2014b, Nonlinear imaging condition to image fractures as nonwelded interface: 84th Annual International Meeting, SEG, Expanded Abstracts, 3905–3909.

Minato, S., and R. Ghose, 2015, Nonlinear imaging condition and effect of source illumination: Imaging fractures as nonwelded interfaces: Geophysics, **80**, no. 2, A25–A30. http://dx.doi.org/10.1190/geo2014-0406.1.

Nakagawa, S., K. Nihei, and R. Myer, 2004, Plane-wave solution for elastic wave scattering by a heterogeneous fracture: The Journal of the Acoustical Society of America, **115**, no. 6, 2761–2772. http://dx.doi.org/10.1121/1.1739483.

Pyrak-Nolte, L., L. Myer, and N. Cook, 1990, Transmission of seismic waves across single natural fractures: Journal of Geophysical Research, **95**, B6, 8617–8638. http://dx.doi.org/10.1029/JB095iB06p08617.

Schoenberg, M., 1980, Elastic wave behavior across linear slip interfaces: The Journal of the Acoustical Society of America, **68**, no. 5, 1516–1521. http://dx.doi.org/10.1121/1.385077.

Wapenaar, K., E. Slob, and J. Fokkema, 2004, Reciprocity and power balance for piecewise continuous media with imperfect interfaces: Journal of Geophysical Research, **109**, B10, B10301. http://dx.doi.org/10.1029/2004JB003002.

Wapenaar, K., J. Thorbecke, J. van der Neut, F. Broggini, E. Slob, and R. Snieder, 2014a, Green's function retrieval from reflection data, in absence of a receiver at the virtual source position: The Journal of the Acoustical Society of America, **135**, no. 5, 2847–2861. http://dx.doi.org/10.1121/1.4869083 PMID:24815266

Wapenaar, K., J. Thorbecke, J. van der Neut, F. Broggini, E. Slob, and R. Snieder, 2014b, Marchenko imaging: Geophysics, **79**, no. 3, WA39–WA57. http://dx.doi.org/10.1190/geo2013-0302.1.

Worthington, M. H., and R. Lubbe, 2007, The scaling of fracture compliance: Geological Society Special Publications, **270**, no. 1, 73–82. http://dx.doi.org/10.1144/GSL.SP.2007.270.01.05.